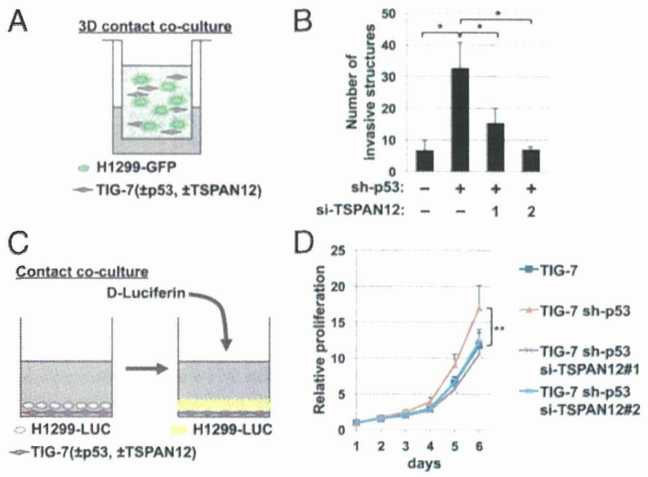

Fig. 4. TSPAN12 regulated cancer cell invasiveness and proliferation enhanced by p53-depleted fibroblasts. (*A*) Scheme of the contact coculture system using a three-dimensional invasion assay. (*B*) TSPAN12 knockdown in p53-depleted TIG-7 cells inhibited invasiveness in H1299-GFP cells. H1299-GFP cells were cocultured with either parental TIG-7 cells, p53-depleted TIG-7 cells, or TIG-7 cells depleted of both p53 and TSPAN12 in Matrigel. After 4 or 5 d, invaded H1299-GFP cells were observed and quantified. (*C*) Scheme of the contact coculture system for a cell proliferation assay. (*D*) TSPAN12 knockdown in p53-depleted TIG-7 cells inhibited proliferation in H1299-LUC cells. H1299-LUC cells were cocultured with either parental TIG-7 cells, p53-depleted TIG-7 cells, or TIG-7 cells depleted of both p53 and TSPAN12. Luciferase activity was measured every day until day 6. Data are the mean ± SD of three or more independent experiments. Statistical analyses were performed using the Student *t* test. $*P < 0.05$, $**P < 0.01$.

Western blotting (Fig. 5*B*). Using these cells, we determined whether p53-depleted fibroblasts enhanced tumor growth in mice. H1299-LUC cells mixed with parental TIG-7 cells were injected into the left back, and H1299-LUC cells mixed with p53-depleted TIG-7 cells were injected into the right back. Tumor growth was greater by H1299-LUC cells with p53-depleted TIG-7 cells than by H1299-LUC cells with parental TIG-7 cells (Fig. 5*C* and Fig. S7*A*). We then examined whether TSPAN12 derepression was required for enhanced tumor growth. TSPAN12 knockdown in p53-depleted fibroblasts suppressed tumor growth in H1299-LUC cells (Fig. 5*D* and Fig. S7*B*). These results demonstrated that stroma-derived TSPAN12 was a critical factor for enhancing tumor growth by p53-depleted fibroblasts.

TSPAN12 in Fibroblasts Promoted CXCL6 Secretion Through the β-Catenin Signaling Pathway to Increase Cancer Cell Invasion. TSPAN12 regulates the Norrin/β-catenin signaling pathway by binding to Frizzled-4, a WNT/Norrin receptor. Therefore, we evaluated the effects of β-catenin knockdown in fibroblasts on cancer cell invasiveness. The knockdown efficiency of siRNAs targeting β-catenin (si–β-catenin) was confirmed by qRT-PCR (Fig. S8*A*) and immunoblotting (Fig. S8*B*). Coculturing H1299-GFP cells with p53-depleted TIG-7 cells transfected with si–β-catenin in Matrigel had less ability to elicit the invasion of H1299-GFP cells than control p53-depleted TIG-7 cells (Fig. 6*A*). To further elucidate the mechanism by which TSPAN12 in fibroblasts enhanced cell invasion, we extracted genes regulated by both p53 and TSPAN12, which may function in cancer cell proliferation, invasion, and metastasis, using the microarray dataset in Fig. S4*A*. The expression levels of these genes were analyzed by semiquantitative RT-PCR. CXCL6 expression was down-regulated by TSPAN12 knockdown (Fig. S8*C*) and was confirmed by qRT-PCR (Fig. 6*B*). The production of CXCL6 secreted from fibroblasts was suppressed by TSPAN12 knockdown, as determined by ELISA (Fig. 6*C*). The knockdown of β-catenin also decreased the expression (Fig. 6*D*) and secretion of CXCL6 (Fig. 6*E*). We next examined whether CXCL6 produced from fibroblasts influenced cancer cell invasiveness. The decreased expression of CXCL6 in TIG-7 cells by si-RNAs was confirmed by qRT-PCR (Fig. S8*D*) and ELISA (Fig. S8*E*), and siRNA-treated cells were cocultured with H1299-GFP cells in Matrigel. Similar to the knockdown of TSPAN12 and β-catenin, that of CXCL6 in p53-depleted TIG-7 cells inhibited the invasiveness of H1299-GFP cells (Fig. 6*F*). The treatment of TIG-7 cells with nutlin-3, a p53 activator, decreased the expression of TSPAN12 (Fig. S8*F*) and CXCL6 (Fig. S8*G*). Although CXCL6 expression was moderately up-regulated by ectopic TSPAN12 expression (Fig. S8 *H* and *I*), its level did not reach that achieved by p53 knockdown, suggesting that further factors are required for the complete up-regulation of CXCL6. Neutralizing antibodies against CXCL6 also inhibited H1299-GFP invasiveness enhanced by coculturing with p53-depleted TIG-7 cells (Fig. 6*G*). The microarray dataset from the Oncomine database (30) revealed that the expression levels of β-catenin (Fig. S9 *A* and *B*) and CXCL6 (Fig. S9 *C* and *D*) were significantly higher in cancer-associated stromal cells than in normal stromal cells. These results suggested that TSPAN12 was required to increase cancer cell invasiveness caused by fibroblasts and orchestrated the transduction of not only cell-to-cell contact-dependent signaling, but also paracrine signaling.

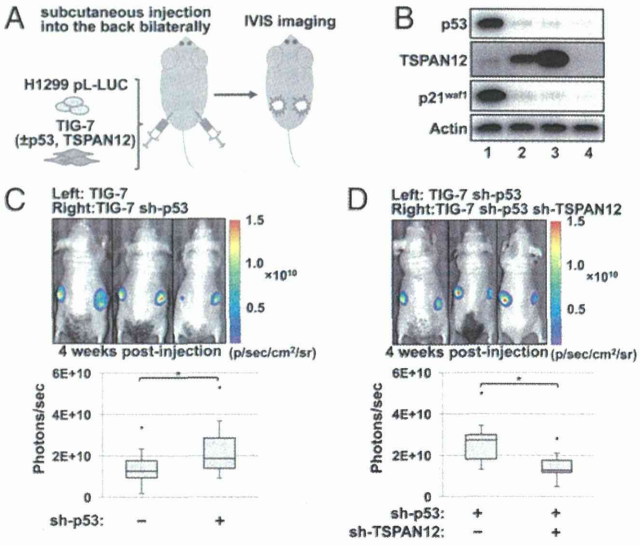

Fig. 5. Knockdown of TSPAN12 derepressed in p53-depleted fibroblasts suppressed cancer cell growth enhanced by coculturing with p53-depleted fibroblasts. (*A*) Scheme of the experimental design to evaluate cancer cell growth coinjected with fibroblasts. H1299-LUC cells mixed with parental TIG-7 cells, p53-depleted TIG-7 cells, or TIG-7 cells depleted of both p53 and TSPAN12 were s.c. injected into the backs of BALB/c-nu/nu mice. Cancer cell growth was quantified using the IVIS imaging system. (*B*) Efficiency of p53 and TSPAN12 knockdown in TIG-7 cells. TIG-7 cells were infected with the indicated viruses and the expression levels of proteins were determined by immunoblotting. Lane 1, parental TIG-7 cells; lane 2, TIG-7 cells expressing sh-p53; lane 3, control of TIG-7 cells expressing sh-p53; lane 4, TIG-7 cells expressing sh-p53 and sh-TSPAN12. (*C*) p53-depleted TIG-7 cells promoted cancer cell growth. Four weeks after the inoculation, cancer cell growth was measured using the IVIS imaging system. (*Left* back) Coinjection with parental TIG-7 cells. (*Right* back) Coinjection with p53-depleted TIG-7 cells ($n = 8$ per group, paired *t* test $*P < 0.05$). (*D*) The depletion of both p53 and TSPAN12 in TIG-7 cells inhibited cancer cell growth increased by p53 depletion in TIG-7 cells. Four weeks after the inoculation, cancer cell growth was measured using the IVIS imaging system. (*Left* back) Coinjection with p53-depleted TIG-7 cells. (*Right* back) Coinjection with TIG-7 cells depleted of both p53 and TSPAN12 ($n = 9$ per group, paired *t* test $*P < 0.05$).

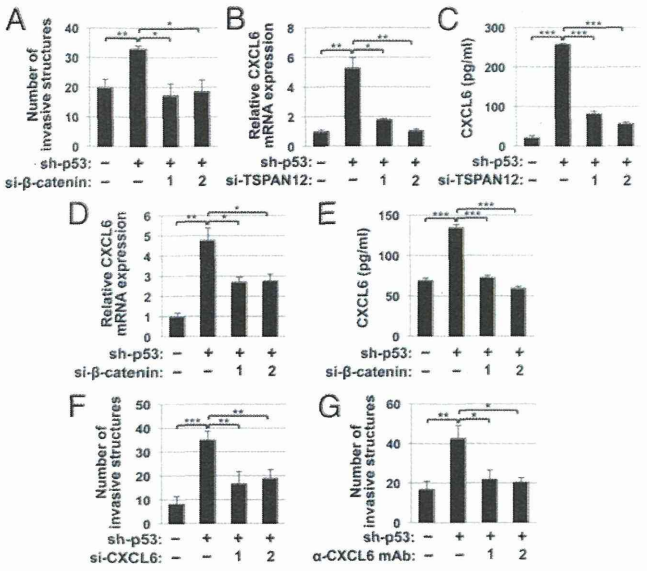

Fig. 6. TSPAN12 promoted CXCL6 expression through the β-catenin signaling pathway. (*A*) β-Catenin knockdown in p53-depleted TIG-7 cells inhibited invasiveness in H1299-GFP cells. H1299-GFP cells were cocultured with parental TIG-7 cells, p53-depleted TIG-7 cells, or TIG-7 cells depleted of both p53 and β-catenin in Matrigel. After 4 or 5 d, invaded H1299-GFP cells were observed under a fluorescent microscope and quantified by counting GFP-positive cells. (*B–E*) TSPAN12 knockdown decreased CXCL6 expression through the β-catenin–mediated pathway. CXCL6 expression was decreased by the knockdown of TSPAN12 and β-catenin. p53-depleted TIG-7 cells were transfected with control siRNAs, si-TSPAN12, or si–β-catenin. CXCL6 expression in cells depleted of TSPAN12 (*B*) or β-catenin (*D*) was determined by qRT-PCR. The production of CXCL6 secreted from cells depleted of TSPAN12 (*C*) or β-catenin (*E*) was quantified by ELISA. (*F*) CXCL6 knockdown in p53-depleted TIG-7 cells canceled fibroblast-elicited invasiveness in H1299-GFP cells. H1299-GFP cells were cocultured with parental TIG-7 cells, p53-depleted TIG-7 cells, or TIG-7 cells depleted of both p53 and CXCL6 in Matrigel. After 4 or 5 d, invaded H1299-GFP cells were observed under a fluorescent microscope and quantified by counting GFP-positive cells. (*G*) Neutralizing antibodies against CXCL6 inhibited invasiveness in H1299-GFP cells. H1299-GFP cells were cocultured with either parental TIG-7 cells or p53-depleted TIG-7 cells, and control IgG or an anti-CXCL6 antibody was added. Four to 5 d after the treatment with these antibodies, invaded H1299-GFP cells were observed under a fluorescent microscope and quantified by counting GFP-positive cells. Data are the mean ± SD of three or more independent experiments. Statistical analyses were performed using the Student *t* test. $*P < 0.05$, $**P < 0.01$, $***P < 0.001$.

Discussion

Fibroblasts are the principal components of connective tissue and function to maintain the homeostasis of ECM and adjacent epithelia (5). CAFs include several mesenchymal cells, including myofibroblast-like cells and normal fibroblasts altered by factors secreted from cancer cells (5, 6). Previous studies reported that mutations in the p53 gene and decreased p53 expression in CAFs, implying functional defects in p53, contributed to cancer progression (14–18). We herein found that culturing fibroblasts with conditioned medium derived from cancer cells suppressed p53 expression in fibroblasts, consistent with the previous finding that epithelial cancer cells suppressed the induction of p53 in neighboring fibroblasts (18). Communication between cancer and stromal cells may be mediated by secreted proteins, including growth factors and cytokines (1–3). However, the mechanism by which p53 expression in stromal cells is regulated by proteins secreted from cancer cells currently remains unknown. One possibility is that TGF-β contributes to the down-regulation of p53 because it activates normal fibroblasts to support cancer and repress p53 expression through the induction of MDM2 (31, 32). Alternatively, cancer-derived exosomes may also be involved in down-regulating p53 expression in stromal cells because cancer cells release exosomes expressing specific proteins and RNAs to influence the expression of various proteins (33, 34). We here demonstrate that α-SMA expression was derepressed by the down-regulation of p53 and negatively correlated with p53 expression levels in stromal tissues from cancer patients. α-SMA is a well-known marker of CAFs (6) and our results suggest that the down-regulation of p53 is, at least in part, involved in the acquisition of a CAF-like phenotype. Genetic studies reported various genetic alterations, including LOH and mutations, in CAFs (2), and our results supported not only p53 mutations and LOH, but also alterations in p53 expression levels contributing to the transition of fibroblasts possessing CAF-like properties from normal fibroblasts.

We focused on the mechanism by which stromal fibroblasts enhanced cancer progression and found that p53-depleted fibroblasts possessing CAF-like properties enhanced cancer cell proliferation and invasion more efficiently than normal fibroblasts. Furthermore, TSPAN12 was identified as a critical factor derepressed by the down-regulation of p53, and TSPAN12 in fibroblasts promoted cancer cell proliferation and invasion through direct cancer-to-stromal cell contact. It still remains unclear how TSPAN12 in fibroblasts promotes cancer cell invasion and proliferation; however, it may bind to other membrane proteins in the transmembrane of neighboring cancer cells and activate a signaling cascade in both fibroblasts and cancer cells because tetraspanin family proteins function as scaffold factors to assemble cell-surface proteins transducing various signals. Although it was not straightforward to elucidate this mechanism, recent studies found that TSPAN12 functioned in the regulation of the Norrin/β-catenin signaling pathway (26). TSPAN12 in fibroblasts regulated CXCL6 expression through the β-catenin–mediated pathway. Therefore, we speculated that TSPAN12 may activate the β-catenin signaling pathway upon binding to a certain membrane protein on cancer cells to promote CXCL6 expression, although certain factors, including SDF-1 (CXCL12), a key tumorigenic factor secreted from p53-depleted

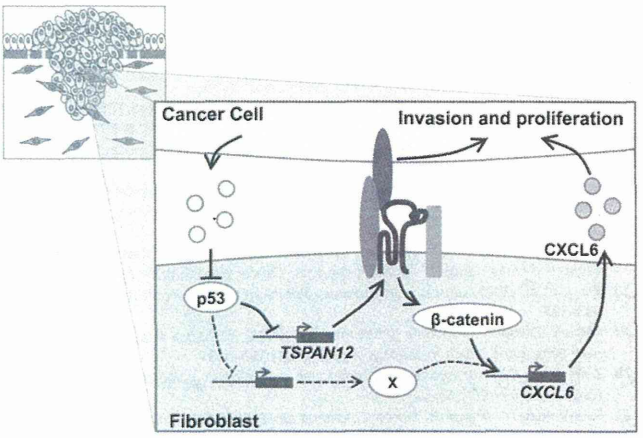

Fig. 7. A model of enhanced cancer invasiveness and proliferation elicited by adjacent fibroblasts. Cancer cells produce various secreted factors, including growth factors, cytokines, and chemokines, and these soluble factors presumably suppress p53 expression in fibroblasts, leading to the up-regulated expression of α-SMA, a marker of CAF-like characteristics. The down-regulation of p53 in fibroblasts derepresses TSPAN12 expression, and TSPAN12 is required to enhance cancer invasiveness and proliferation elicited by p53 down-regulated fibroblasts through contact between cancer cells and fibroblasts. The up-regulated expression of TSPAN12 promotes CXCL6 expression through the β-catenin–mediated pathway, which leads to enhanced cancer progression.

fibroblasts (13, 35), and transmembrane proteins that interact with cancer cells, may also contribute to fibroblast-elicited cancer progression (Fig. 7). We cannot exclude the possibility that TSPAN12 in fibroblasts may enhance the creation of tunnels by destroying ECM, enabling cancer cells to follow through their contact with fibroblasts (36). Further investigations of these issues will be required to elucidate the role of TSPAN12 in cancer progression.

Genes that are derepressed by the down-regulation of p53, such as MDR1 (37), CD44 (38), TCTP (39), and TSPAN2 (40), have been identified, and we found that TSPAN12 was derepressed by the down-regulation of p53 in fibroblasts. The mechanism underlying the transcriptional derepression of TSPAN12 through the down-regulation of p53 is complex, and even though a reporter assay using the TSPAN12 promoter region (−1,000 to −1) and ChIP analysis of the proximal TSPAN12 promoter region (−230 to −1) using various specific primers were conducted, we could not confirm that TSPAN12 was a direct p53-target gene. One reason is that p53 may block the recruitment of some coactivators to the TSPAN12 promoter by binding p53 to these coactivators (41). Alternatively, TSPAN12 expression may be regulated by p53 through the inhibition of p53-distal enhancer activity because p53 suppresses the expression of many genes in embryonic stem (ES) cells and influences the *cis* element far from promoter regions (42). However, further investigations will be required to elucidate how p53 regulates TSPAN12 expression. Cancer-associated stromal cells were recently recognized as an effective target for cancer therapy (43–45), and the recombinant soluble extracellular region of TSPAN12, antibodies against TSPAN12 and CXCL6, may become effective therapeutic agents.

Materials and Methods

Cell cultures and the immunoblotting analysis were performed as described in Endo et al. (46). *SI Materials and Methods* include detailed additional information on cell cultures, viral infection, plasmid construction, antibodies, siRNA transfection, and immunoblot analysis, as well as descriptions on quantitative and semiquantitative RT-PCR, the ELISA, invasion assay, proliferation assay, Transwell migration assay in coculture, microarray analysis, production and purification of large extracellular loops of TSPAN12, tumor growth assay, and statistical analysis.

ACKNOWLEDGMENTS. We thank Dr. Teruhiko Yoshida and Ms. Sachiyo Mimaki for expression profiling. This work was supported in part by Grants-in-Aid from the Ministry of Health, Labor and Welfare for the Third Term Comprehensive 10-Year Strategy for Cancer Control, and the National Cancer Center Research and Development Fund 23-B-27(23-A-37) (to M.E.) and 23-A-7 (to core facility).

1. Mueller MM, Fusenig NE (2004) Friends or foes: Bipolar effects of the tumour stroma in cancer. *Nat Rev Cancer* 4(11):839–849.
2. Polyak K, Haviv I, Campbell IG (2009) Co-evolution of tumor cells and their microenvironment. *Trends Genet* 25(1):30–38.
3. Quail DF, Joyce JA (2013) Microenvironmental regulation of tumor progression and metastasis. *Nat Med* 19(11):1423–1437.
4. Bhowmick NA, Neilson EG, Moses HL (2004) Stromal fibroblasts in cancer initiation and progression. *Nature* 432(7015):332–337.
5. Kalluri R, Zeisberg M (2006) Fibroblasts in cancer. *Nat Rev Cancer* 6(5):392–401.
6. Madar S, Goldstein I, Rotter V (2013) 'Cancer associated fibroblasts'—more than meets the eye. *Trends Mol Med* 19(8):447–453.
7. Olumi AF, et al. (1999) Carcinoma-associated fibroblasts direct tumor progression of initiated human prostatic epithelium. *Cancer Res* 59(19):5002–5011.
8. Vousden KH, Prives C (2009) Blinded by the light: The growing complexity of p53. *Cell* 137(3):413–431.
9. Menendez D, Inga A, Resnick MA (2009) The expanding universe of p53 targets. *Nat Rev Cancer* 9(10):724–737.
10. Bar J, Moskovits N, Oren M (2010) Involvement of stromal p53 in tumor-stroma interactions. *Semin Cell Dev Biol* 21(1):47–54.
11. Shimoda M, Mellody KT, Orimo A (2010) Carcinoma-associated fibroblasts are a rate-limiting determinant for tumour progression. *Semin Cell Dev Biol* 21(1):19–25.
12. Kiaris H, et al. (2005) Evidence for nonautonomous effect of p53 tumor suppressor in carcinogenesis. *Cancer Res* 65(5):1627–1630.
13. Addadi Y, et al. (2010) p53 status in stromal fibroblasts modulates tumor growth in an SDF1-dependent manner. *Cancer Res* 70(23):9650–9658.
14. Kurose K, et al. (2002) Frequent somatic mutations in PTEN and TP53 are mutually exclusive in the stroma of breast carcinomas. *Nat Genet* 32(3):355–357.
15. Patocs A, et al. (2007) Breast-cancer stromal cells with TP53 mutations and nodal metastases. *N Engl J Med* 357(25):2543–2551.
16. Fukino K, Shen L, Patocs A, Mutter GL, Eng C (2007) Genomic instability within tumor stroma and clinicopathological characteristics of sporadic primary invasive breast carcinoma. *JAMA* 297(19):2103–2111.
17. Hawsawi NM, et al. (2008) Breast carcinoma-associated fibroblasts and their counterparts display neoplastic-specific changes. *Cancer Res* 68(8):2717–2725.
18. Bar J, et al. (2009) Cancer cells suppress p53 in adjacent fibroblasts. *Oncogene* 28(6):933–936.
19. Serru V, Dessen P, Boucheix C, Rubinstein E (2000) Sequence and expression of seven new tetraspans. *Biochim Biophys Acta* 1478(1):159–163.
20. Zöller M (2009) Tetraspanins: Push and pull in suppressing and promoting metastasis. *Nat Rev Cancer* 9(1):40–55.
21. Sala-Valdés M, Ailane N, Greco C, Rubinstein E, Boucheix C (2012) Targeting tetraspanins in cancer. *Expert Opin Ther Targets* 16(10):985–997.
22. Hemler ME (2005) Tetraspanin functions and associated microdomains. *Nat Rev Mol Cell Biol* 6(10):801–811.
23. Yáñez-Mó M, Barreiro O, Gordon-Alonso M, Sala-Valdés M, Sánchez-Madrid F (2009) Tetraspanin-enriched microdomains: A functional unit in cell plasma membranes. *Trends Cell Biol* 19(9):434–446.
24. Nikopoulos K, et al. (2010) Next-generation sequencing of a 40 Mb linkage interval reveals TSPAN12 mutations in patients with familial exudative vitreoretinopathy. *Am J Hum Genet* 86(2):240–247.
25. Poulter JA, et al. (2010) Mutations in TSPAN12 cause autosomal-dominant familial exudative vitreoretinopathy. *Am J Hum Genet* 86(2):248–253.
26. Junge HJ, et al. (2009) TSPAN12 regulates retinal vascular development by promoting Norrin- but not Wnt-induced FZD4/beta-catenin signaling. *Cell* 139(2):299–311.
27. Xu D, Sharma C, Hemler ME (2009) Tetraspanin12 regulates ADAM10-dependent cleavage of amyloid precursor protein. *FASEB J* 23(11):3674–3681.
28. Knoblich K, et al. (2014) Tetraspanin TSPAN12 regulates tumor growth and metastasis and inhibits β-catenin degradation. *Cell Mol Life Sci* 71(7):1305–1314.
29. Hemler ME (2014) Tetraspanin proteins promote multiple cancer stages. *Nat Rev Cancer* 14(1):49–60.
30. Finak G, et al. (2008) Stromal gene expression predicts clinical outcome in breast cancer. *Nat Med* 14(5):518–527.
31. Araki S, et al. (2010) TGF-beta1-induced expression of human Mdm2 correlates with late-stage metastatic breast cancer. *J Clin Invest* 120(1):290–302.
32. López-Díaz FJ, et al. (2013) Coordinate transcriptional and translational repression of p53 by TGF-β1 impairs the stress response. *Mol Cell* 50(4):552–564.
33. D'Souza-Schorey C, Clancy JW (2012) Tumor-derived microvesicles: Shedding light on novel microenvironment modulators and prospective cancer biomarkers. *Genes Dev* 26(12):1287–1299.
34. Kharaziha P, Ceder S, Li Q, Panaretakis T (2012) Tumor cell-derived exosomes: A message in a bottle. *Biochim Biophys Acta* 1826(1):103–111.
35. Moskovits N, Kalinkovich A, Bar J, Lapidot T, Oren M (2006) p53 Attenuates cancer cell migration and invasion through repression of SDF-1/CXCL12 expression in stromal fibroblasts. *Cancer Res* 66(22):10671–10676.
36. Brentnall TA, et al. (2012) Arousal of cancer-associated stroma: overexpression of palladin activates fibroblasts to promote tumor invasion. *PLoS ONE* 7(1):e30219.
37. Johnson RA, Ince TA, Scotto KW (2001) Transcriptional repression by p53 through direct binding to a novel DNA element. *J Biol Chem* 276(29):27716–27720.
38. Godar S, et al. (2008) Growth-inhibitory and tumor- suppressive functions of p53 depend on its repression of CD44 expression. *Cell* 134(1):62–73.
39. Amson R, et al. (2012) Reciprocal repression between P53 and TCTP. *Nat Med* 18(1):91–99.
40. Otsubo C, et al. (2014) TSPAN2 is involved in cell invasion and motility during lung cancer progression. *Cell Reports* 7(2):527–538.
41. Böhlig L, Rother K (2011) One function—multiple mechanisms: The manifold activities of p53 as a transcriptional repressor. *J Biomed Biotechnol* 2011:464916.
42. Li M, et al. (2012) Distinct regulatory mechanisms and functions for p53-activated and p53-repressed DNA damage response genes in embryonic stem cells. *Mol Cell* 46(1):30–42.
43. Gonda TA, Varro A, Wang TC, Tycko B (2010) Molecular biology of cancer-associated fibroblasts: Can these cells be targeted in anti-cancer therapy? *Semin Cell Dev Biol* 21(1):2–10.
44. Bissell MJ, Hines WC (2011) Why don't we get more cancer? A proposed role of the microenvironment in restraining cancer progression. *Nat Med* 17(3):320–329.
45. Junttila MR, de Sauvage FJ (2013) Influence of tumour micro-environment heterogeneity on therapeutic response. *Nature* 501(7467):346–354.
46. Endo Y, et al. (2008) Regulation of clathrin-mediated endocytosis by p53. *Genes Cells* 13(4):375–386.

Supporting Information

Otomo et al. 10.1073/pnas.1412062112

SI Materials and Methods

Cell Culture. Human lung cancer cell lines (H1299, H460, and A549) were maintained in RPMI medium 1640 (Sigma-Aldrich) supplemented with 10% (vol/vol) FBS (Gibco), penicillin (100 units/mL) (Sigma-Aldrich), and streptomycin (100 units/mL) (Sigma-Aldrich) at 37 °C in a 5% (vol/vol) CO_2 incubator. Human embryonic lung fibroblast cell lines (TIG-7 and WI-38) were maintained in DMEM (Sigma-Aldrich) supplemented with 10% (vol/vol) FBS, penicillin (100 units/mL), and streptomycin (100 units/mL) at 37 °C in a 5% (vol/vol) CO_2 incubator. Immortalized small airway epithelial cells (SAECs) were generated and maintained as described previously (1).

Viral Infection. Retroviral production and infection were performed as described previously (1). Briefly, the day before transfection, Phoenix-Ampho cells (5×10^6) were seeded in 100-mm tissue culture dishes. The next day, retroviral vectors were transfected using Lipofectamine 2000 reagent (Invitrogen), according to the manufacturer's protocol. Culture media were replaced 6 h after transfection, incubated at 37 °C for 48 h, and retrovirus-containing supernatants were collected from culture media. TIG-7 cells were plated in tissue culture dishes and infected with retroviruses in media containing 4 μg/mL Polybrene (Sigma-Aldrich). After being infected, media containing retroviruses were replaced with fresh media and, 2 d after infection, culture media were changed to media containing 0.5 μg/mL puromycin (Sigma-Aldrich).

Lentiviral production and infection were performed as described previously (1). Briefly, the ViraPower Lentiviral Expression System (Invitrogen) was used to produce lentiviruses according to the manufacturer's protocol, and infected cells were selected using 4 μg/mL (for TIG-7 and WI-38) or 10 μg/mL (for H1299) Blasticidin S (Invitrogen).

Plasmid Construction. The construction of pSR-53 and pSL-p53 was described previously (2). To construct pLenti-shTSPAN12 (pSL-TSPAN12), the following oligonucleotides containing target sequences were annealed and ligated into the pSUPER.retro vector (Oligoengine): shTSPAN12, 5′-GATCCCCGCTTATCTTTGCCTTCTCCTTCAAGAGAGGAGAAGGCAAAGATAAGCTTTTTGGAAA-3′ and 5′-AGCTTTTCCAAAAAGCTTATCTTTGCCTTCTCCTCTTGAAGGAGAAGGCAAAGATAAGCGGG-3′. Target sequences containing the H1 promoter were digested from the above plasmid (pSR-TSPAN12) and ligated into the pLenti6/V5-DEST vector (Invitrogen). To construct pLenti-TSPAN12-FHH, cDNA fragments encoding TSPAN12 were amplified by PCR using the following primers: 5′-CCGGATCCATGGCCAGAGAAGATTCCGTG-3′ and 5′-CCGCTCGAGTAACTCCTCCATCTCAAAGTGT-3′. The PCR fragment was digested with BamHI and XhoI and inserted into the pcDNA3.1-FHH (FLAG-HA-His) plasmid. The TSPAN12 fragment containing the FHH tag was digested from the above plasmid (pcDNA3.1-TSPAN12-FHH) and ligated into the pLenti6/V5-DEST vector (Invitrogen). To construct pFUSE-TSPAN12-LEL-Fc and pFUSE-TSPAN12-LEL-VR-Fc, cDNA fragments encoding TSPAN12-LEL and TSPAN12-LEL-VR were amplified by PCR using the following primers: TSPAN12-LEL, 5′-GGCCATGGTTGGCGTTTGGACATATGAACAGGAAC-3′ and 5′-GCCGGATCCGCTCTGAAAGTACAGATCCTCCCTCAGCACCTGCAGTTGTTTGG-3′; TSPAN12-LEL-VR, 5′-GGCCATGGTTTGCTGTGGAGTAGTATATTTCACTG-3′ and 5′-GCCGGATCCGCTCTGAAAGTACAGATCCTCACAACCCTCTTGATAAAGGTCAC-3′. PCR fragments were digested with NcoI and BamHI and inserted into the pFUSE-hIgG4-Fc2 vector (InvivoGen) digested with NcoI and BglII.

Antibodies. Anti-p53 antibody (DO-1)-conjugated horseradish peroxidase and an antiactin antibody were purchased from Santa Cruz Biotechnology. The anti-$p21^{waf1}$ antibody was from Epitomics. The anti–β-catenin antibody was from Cell Signaling Technology. The anti–α-tubulin and anti–α-smooth muscle actin antibodies were from Sigma-Aldrich. The anti-CXCL6 antibody and mouseIgG1 isotype control were from R&D Systems. Another anti-CXCL6 antibody was from Novus Biologicals. An anti-TSPAN12 antibody was generated by immunizing with rabbits the C-terminal peptides of TSPAN12 (EHTSMANSFNTHFEMEEL) and immunized antiserum was affinity purified.

siRNA Transfection. siRNA duplexes were purchased from Sigma-Aldrich (for TSPAN12, β-catenin, and CXCL6) and Invitrogen (for p53). The sequences of siRNA duplexes were as follows: si-TSPAN12#1, 5′-GCUUAUCUUUGCCUUCUCCTT-3′ and 5′-GGAGAAGGCAAAGAUAAGCTT-3′; si-TSPAN12#2, 5′-AUGAGGGACUACCUAAAUATT-3′ and 5′-UAUUUAGGUAGUCCCUCAUTT-3′; si-β-catenin#1, 5′-GGAUGUUCACAACCGAAUUTT-3′ and 5′-AAUUCGGUUGUGAACAUCCTT-3′; si-β-catenin#2, 5′-CCACUAAUGUCCAGCGUUUTT-3′ and 5′-AAACGCUGGACAUUAGUGGTT-3′; si-CXCL6#1, 5′-GGAGGUAUCCUGUUGUUCUTT-3′ and 5′-AGAACAACAGGAUACCUCCTT-3′; si-CXCL6#2, 5′-CGCGUUACGCUGAGAGUAATT-3′ and 5′-UUACUCUCAGCGUAACGCGTT-3′; si-p53#1, 5′-UUAACCCUCACAAUGCACUCUGUGA-3′ and 5′-UCACAGAGUGCAUUGUGAGGGUUAA-3′; si-p53#2, 5′-CCAUCCACUACAACUACAUGUGUAA-3′ and 5′-UUACACAUGUAGUUGUAGUGGAUGG-3′. The transfection of siRNAs in fibroblasts was performed using Lipofectamine 2000 (Invitrogen) or Lipofectamine RNAiMAX (Invitrogen) according to the manufacturer's protocol.

Immunoblot Analysis. To produce conditioned medium, lung cancer cells (2×10^6) were seeded on 100-mm dishes and conditioned medium was collected after 48 h. Fibroblasts (2×10^5) were seeded on six-well plates and treated with conditioned medium or transfected with siRNAs. After 24–72 h, cells were harvested, washed with PBS, and lysed with lysis buffer [50 mM Tris·HCl (pH 7.2), 250 mM NaCl, 2 mM $MgCl_2$, 0.1 mM EDTA, 0.1 mM EGTA, and 0.1% Nonidet P-40] containing proteinase inhibitor mixture (Roche), 10 mM NaF, 1 mM Na_3VO_4, and 1 mM DTT. After being incubation for 30 min on ice, lysates were centrifuged at $20,000 \times g$ for 15 min and the supernatants collected were mixed with SDS/PAGE sample buffer. The samples were then boiled for 5 min and resolved by 5–20% (wt/vol) SDS/PAGE. After electrophoresis, the proteins were transferred to a PVDF membrane (Millipore), blocked with 5% (wt/vol) nonfat milk in TBST [20 mM Tris·HCl (pH 7.6), 137 mM NaCl, 0.1% Tween-20], and probed with primary antibodies at room temperature for 1 h. The blots were then washed, exposed to HRP-conjugated secondary antibodies (1:5,000 dilution) for 1 h, and the antigen–antibody complex was detected by enhanced chemiluminescence (Amersham Pharmacia Biotech).

Quantitative RT-PCR. Total RNA was isolated from cells using the RNeasy mini kit (Qiagen). Two micrograms of total RNA was reverse transcribed with the SuperScript III First-Strand Synthesis system (Invitrogen). Quantitative RT-PCR (qRT-PCR) was

performed using the FastStart Universal SYBR Green master mix (Roche) and analyzed with the 7900HT Fast Real-Time PCR system (Applied Biosystems) or CFX96 Touch Real-Time PCR Detection system (Bio-Rad). The primers for qRT-PCR were as follows: 5′-GTGAAGGTCGGAGTCAACG-3′ and 5′-TGAGGTCAATGAAGGGGTC-3′ for GAPDH; 5′-TAGTGTGGTGGTGCCCTATGAG-3′ and 5′-AGTGTGATGATGGTGAGGATGG-3′ for p53; 5′-TGATTAGCAGCGGAACAAGG-3′ and 5′-CGTTAGTGCCAGGAAAGACAAC-3′ for $p21^{waf1}$; 5′-TGGGAGTAGGATGTGGTGAAAG-3′ and 5′-AAGAGCAGATTGAGGGCGTAG-3′ for TSPAN12; 5′-CCCACTGGCCTCTGATAAAGG-3′ and 5′-ACGCAAAGGTGCATGATTTG-3′ for β-catenin; and 5′-ATTTCCCCAGCATCCCAAAG-3′ and 5′-CATAGTGGTCAAGAGAGGGTTCG-3′ for CXCL6.

Semiquantitative RT-PCR. Total RNA was isolated from cells using the RNeasy mini kit (Qiagen). Two micrograms of total RNA was reverse transcribed with the SuperScript III First-Strand Synthesis system (Invitrogen). The PCR was performed using Taq DNA Polymerase (1 unit/μL), dNTPPack (Roche) in a PCR thermal cycler (MJ Research, Bio-Rad). The primers for the PCR were as follows: TSPAN12, 5′-ATGGCCAGAGAAGATTCCGTG-3′ and 5′-TTATAACTCCTCCATCTCAAAGT-3′; p53, 5′-AAAGGGGAGCCTCACCACG-3′ and 5′-ACGCACACCTATTGCAAGCAA-3′; $p21^{waf1}$, 5′-AGTGGACAGCGAGCAGCTGAGC-3′ and 5′-GCAGCAGAGCAGGTGAGGTGC-3′; CXCL6, 5′-ATGAGCCTCCCGTCCAGCC-3′ and 5′-TCAGTTTTTCTTGTTTCCACTGT-3′; HGF, 5′-GGTTCTCAATGTTTCCCAGCTG-3′ and 5′-CTATGACTGTGGTACCTTATATG-3′; TFPI2, 5′-ATGGACCCCGCTCGCCCC-3′ and 5′-TTAAAATTGCTTCTTCCGAATTTTC-3′; DLL4, 5′-CTGCTGGTACTGCTGGGCA-3′ and 5′-TTATACCTCCGTGGCAATGAC-3′; TNFRSF19, 5′-GGTTGTGGGGTGCATTCTGC-3′ and 5′-TCACAGGGAACCCAGTCGCT-3′; SALL1, 5′-ACTGCTTGTGACATTTGTGGC-3′ and 5′-TTAACTCGTGACGATCTCCTTG-3′; PTGS1, 5′-GAACATGGACCACCACATCCT-3′ and 5′-TCAGAGCTCTGTGGATGGTC-3′; NCKAP5, 5′-TCCAGTCAG-CCCTTTCTGCA-3′ and 5′-TCAAGTTGTCTCAATTTCTGGG-3′; and GAPDH, 5′-GGGGAGCCAAAAGGGTCATCATCTC-3′ and 5′-TCCACAGTCTTCTGGGTGGCAGTGA-3′. The PCR products were subjected to electrophoresis on a 1% agarose gel containing 0.5 μg/mL ethidium bromide.

ELISA Assay. TIG-7 cells (5×10^4) were seeded on 24-well plates and transfected with siRNAs. Culture medium was replaced 48 h after transfection, further incubated for 48 h, and conditioned medium was then collected. The antigen–antibody reaction was performed using DuoSet ELISA for human CXCL6 (R&D Systems) according to the manufacturer's instructions. Streptavidin–HRP-bound samples were reacted with peroxidase (Sumilon), and measured at an absorbance of 490 nm using a plate reader (PerkinElmer).

Invasion Assay by Coculture in Matrigel. In the contact coculture, H1299-GFP cells (1×10^3) and TIG-7 cells (1×10^3) were suspended in 50 μL of a mixture of DMEM and Matrigel (Becton-Dickinson) (1:1, vol/vol) and layered onto 20 μL of presolidified mixture in a 96-well Transwell plate (Corning). In the noncontact coculture, TIG-7 cells (3×10^3) were seeded on the bottom plate and H1299-GFP cells (1×10^3) were layered onto a 96-well Transwell insert as described above. Culture medium (150 μL) was added to the lower wells and changed every 2–3 d. The anti-CXCL6 antibody (10 μg/mL) or TSPAN12-large extracellular loop (LEL)-Fc protein (10 μg/mL) was added to culture medium and changed every 2 d. Colonies of H1299-GFP cells were observed under a confocal microscope for 4–5 d after culturing and colonies morphologically exhibiting the invasive outgrowth phenotype were counted.

Proliferation Assay by Coculture. In the contact coculture, H1299-LUC cells (3×10^2) were plated onto a monolayer of TIG-7 cells (1×10^3) in a 96-well plate. The next day, 150 μg/mL D-luciferin (Wako) was added to the culture medium and luminescence was measured using a luminometer (PerkinElmer) to monitor the proliferation of H1299-LUC cells. After measuring luminescence, the medium was replaced and, after 24 h, luminescence was measured again. These procedures were repeated five times. In the noncontact coculture using conditioned medium, H1299-LUC cells (3×10^2) and TIG-7 cells (1×10^3) were seeded individually onto a 96-well plate. The next day, medium in H1299-LUC cells was changed to conditioned medium collected from TIG-7 cells. Luciferase activity was measured after 24 h, and medium in H1299-LUC cells was changed to newly conditioned medium from TIG-7 every day for 5 d. In the noncontact coculture using a Transwell insert, H1299-LUC cells (5×10^2) were seeded on a 96-well companion plate and TIG-7 cells (1×10^3) were seeded on a 96-well Transwell insert. After 24 h, the Transwell insert was combined with the companion plate and luciferase activity in H1299-LUC cells 24 h after being incubated was measured using a luminometer. Medium from the companion plate was replaced and luciferase activity in H1299-LUC cells was measured at 24-h intervals.

Transwell Migration Assay in Coculture. In the contact coculture, H1299-GFP cells (5×10^4) were plated with TIG-7 cells (5×10^4) suspended in 500 μL of serum-free DMEM, and then plated onto 8.0-μm pore size 24-well Transwell inserts (Becton-Dickinson). The bottom well was filled with 750 μL of DMEM containing 10% (vol/vol) FBS. After being incubated at 30 °C with 5% (vol/vol) CO_2 for 16 h, the cells on the upper surface of the Transwell insert were scraped using cotton swabs. The migrated cells on the lower surface were observed under a fluorescence microscope.

Microarray Analysis. Total RNA was purified using an RNeasy kit (Qiagen) and subjected to a microarray experiment. Target cRNA was prepared from 5 μg total RNA with a One-Cycle cDNA Synthesis kit and 3′-amplification reagents for IVT Labeling (Affimetrix), and hybridized to GeneChip Human Genome U133 Plus 2.0 arrays (Affimetrix) according to the manufacturer's instructions. The expression value (signal) and change value (signal log ratio) of each gene were calculated and normalized using GeneChip Operating Software version 1.4 (Affimetrix). We performed the experiment in duplicate and selected the genes exhibiting threefold or more changes in both comparisons.

Production and Purification of Large Extracellular Loop of TSPAN12. The 293FT cells were plated at 80–90% confluence the day before transfection and subsequently transfected with pFUSE-TSPAN12-LEL or pFUSE-TSPAN12-LEL-VR or no insert control (pFUSE-Fc) using Lipofectamine 2000 according to the manufacturer's protocol. Conditioned meda were harvested 24–96 h after transfection and debris were removed by centrifugation at $600 \times g$ for 3 min. Soluble proteins were purified with Protein A Sepharose (GE Healthcare) and concentrated using Amicon Ultra 3K (Millipore). To more efficiently collect TSPAN12-LEL, cells were harvested and lysed with lysis buffer (20 mM Hepes-KOH, pH 7.5, 150 mM NaCl, 5 mM $MgCl_2$, 1% CHAPS) 72 h after transfection and subsequently sonicated. TSPAN12-LEL was purified with Protein A Sepharose and concentrated using Amicon Ultra 3K. The concentration of purified proteins was determined with SDS/PAGE and Coomassie Brilliant Blue (CBB) staining.

Tumor Growth Assay. H1299-LUC cells (5×10^5) were mixed with TIG-7 cells (1.5×10^6) in 100 μL DMEM–Matrigel mixture (1:1, vol/vol) and injected s.c. into the backs of BALB/c-nu/nu mice (CREA Japan). Tumor growth was monitored using the IVIS

imaging system (Xenogen). The mouse xenograft study was conducted according to the regulations of the Institutional Animal Care and Use Committee at the National Cancer Center Research Institute, Tokyo Japan.

Statistical Analysis. Data are shown as the means ± SDs of three or more independent experiments. Statistical analyses were performed using the Student t test, paired t test, and Wilcoxon signed-rank test with a significance level of $P < 0.05$.

1. Otsubo C et al. (2014) TSPAN2 is involved in cell invasion and motility during lung cancer progression. *Cell Reports* 7(2):527–538.

2. Endo Y, et al. (2008) Regulation of clathrin-mediated endocytosis by p53. *Genes Cells* 13(4):375–386.

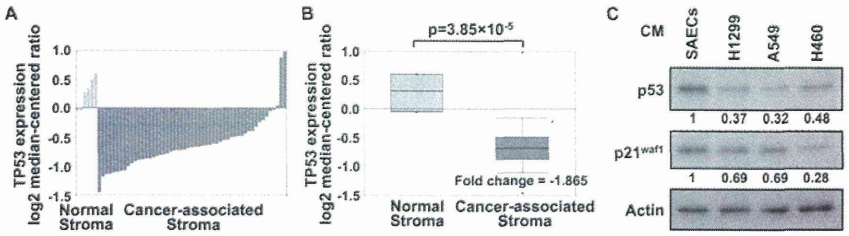

Fig. S1. Expression levels of p53 (TP53) in breast cancer-associated stromal tissues obtained by laser-captured microdissection were lower than those in stromal tissues. (*A* and *B*) Expression levels of p53 in 6 samples of normal stromal tissues and 53 samples of cancer-associated stromal tissues extracted from the Oncomine dataset are shown individually (*A*) and collectively (*B*). (*C*) p53 expression in TIG-7 cells was down-regulated by conditioned medium from cancer cells. TIG-7 cells were treated with conditioned medium for 48 h, and expression levels of the indicated proteins in these cell lysates were determined by immunoblotting and quantified using ImageJ version 1.47c software.

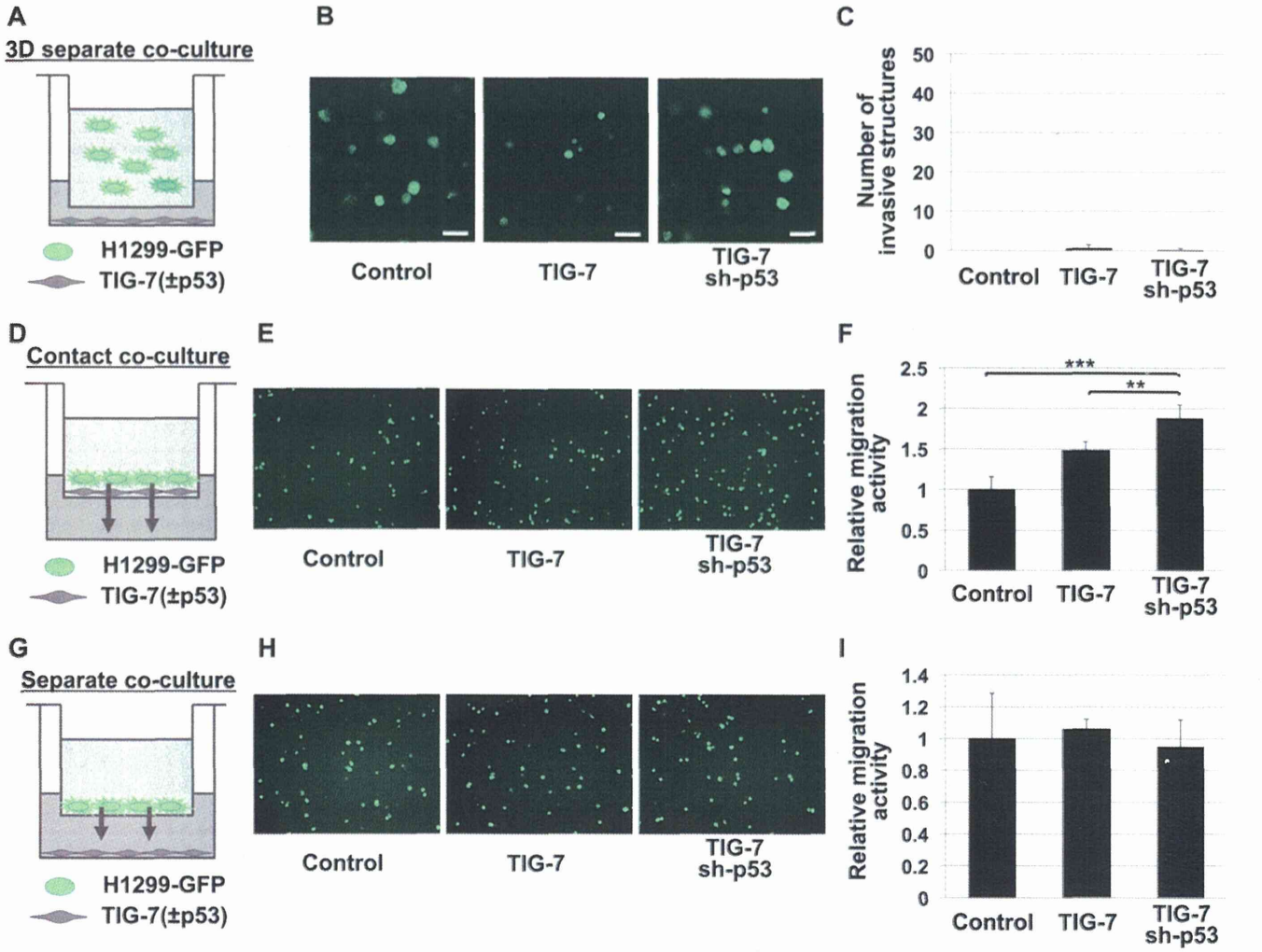

Fig. S2. p53-depleted fibroblasts enhanced the invasion and migration of cancer cells through direct cell-to-cell contact. (*A*) Scheme of the noncontact co-culture system using a three-dimentional invasion assay. (*B* and *C*) p53-depleted TIG-7 cells did not enhance invasiveness in H1299-GFP cells regardless of cell number and confluency using a contact coculture system. Three times as many H1299-GFP cells as in the assays of Fig. 2 *D* and *E* were cocultured with parental TIG-7 cells or p53-depleted TIG-7 cells, or cultured alone in Matrigel. After 4–5 d, H1299-GFP cells were observed under a confocal microscope (*B*). (Scale bar, 100 μm.) Quantification of invasive phenotypic cells in H1299-GFP cells (*C*). (*D*) Scheme of the contact coculture migration assay. (*E* and *F*) p53-depleted TIG-7 cells enhanced migration activity in H1299-GFP cells using the contact coculture system. H1299-GFP cells were cocultured with parental TIG-7 cells or p53-depleted TIG-7 cells, or cultured alone in an 8.0-μm pore Transwell insert. After 16 h, migrated cells were observed under a fluorescence microscope (*E*). Quantification of migrated H1299-GFP cells (*F*). (*G*) Scheme of the noncontact coculture migration assay. (*H* and *I*) p53-depleted TIG-7 cells did not enhance migration activity in H1299-GFP cells using the noncontact coculture system. H1299-GFP cells were plated on an 8.0-μm pore Transwell insert, and parental TIG-7 cells or p53-depleted TIG-7 cells were plated on the bottom well. After 16 h, migrated cells were observed under a fluorescence microscope (*H*). Quantification of migrated H1299-GFP cells (*I*). Data are the mean ± SD of three or more independent experiments. Statistical analyses were performed using the Student *t* test. $^{**}P < 0.01$, $^{***}P < 0.001$.

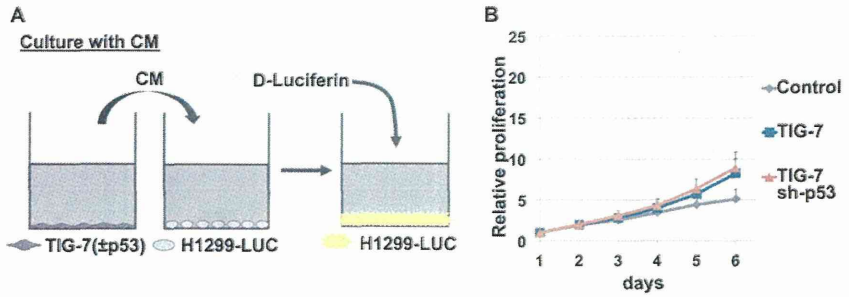

Fig. S3. p53-depleted TIG-7 cells did not enhance cell proliferation in H1299-LUC cells using the noncontact coculture system. (*A*) Scheme of the noncontact coculture system using conditioned medium for the cell proliferation assay. (*B*) The cell proliferation assay using the noncontact coculture system is shown. H1299-LUC cells were treated with conditioned medium from parental TIG-7 cells or p53-depleted TIG-7 cells. Luciferase activity was measured every day until day 6.

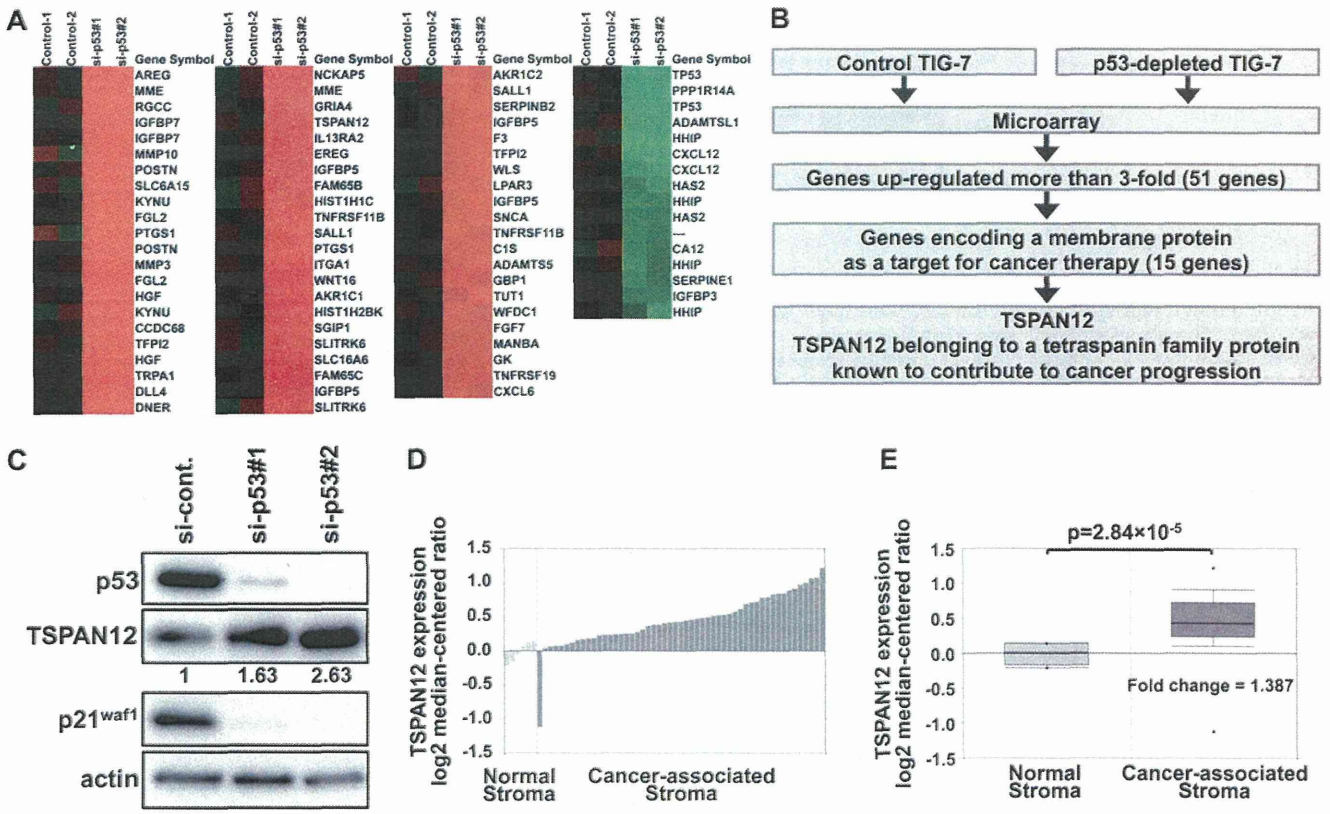

Fig. S4. TSPAN12 was derepressed by p53 knockdown. (*A*) Expression levels altered by p53 knockdown are listed. Microarray experiments were performed using cDNA samples from parental TIG-7 cells or p53-depleted TIG-7 cells. Fifty-one genes were up-regulated (fold change, >3) and 9 genes were down-regulated (fold change, <0.33) in p53-depleted TIG-7 cells. (*B*) Scheme of the identification of TSPAN12. (*C*) TSPAN12 was derepressed by transient p53 knockdown using si-p53. Cell lysates were prepared from fibroblasts transfected with indicated siRNAs and the expression levels of indicated genes were determined by immunoblotting. (*D* and *E*) The expression level of TSPAN12 was higher in breast cancer-associated stromal tissues than in normal stromal tissues. (*D* and *E*) The expression levels of TSPAN12 in 6 samples of normal stromal tissues and 53 samples of cancer-associated stromal tissues extracted from the Oncomine dataset are shown individually (*D*) and collectively (*E*).

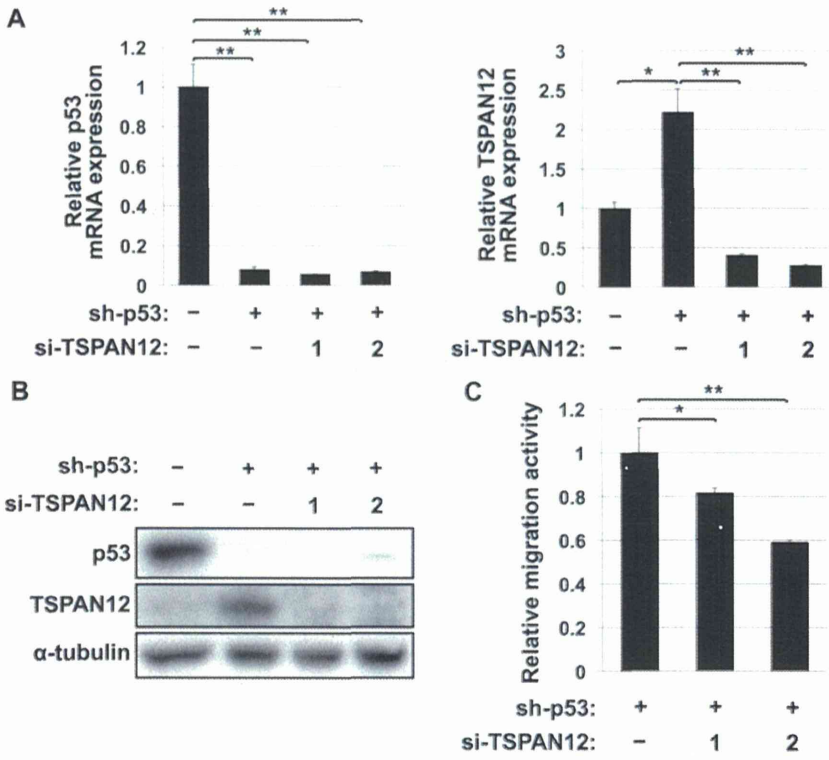

Fig. S5. TSPAN12 regulated the migration activity of cancer cells enhanced by p53-depleted fibroblasts. (*A* and *B*) Efficiency of TSPAN12 knockdown in TIG-7 cells. TIG-7 cells were infected with either control lentiviruses or lentiviruses for the expression of shRNAs against p53 and transfected with control siRNAs or siRNAs against TSPAN12. Expression levels of the indicated genes were determined by qRT-PCR (*A*) and immunoblotting (*B*). (*C*) TSPAN12 knockdown in p53-depleted TIG-7 cells inhibited the migration activity of H1299-GFP cells. H1299-GFP cells were cocultured with either p53-depleted TIG-7 or TIG-7 cells depleted of both p53 and TSPAN12 in an 8.0-μm pore cell culture insert. After 16 h, migrated cells were observed and quantified. Data are the mean ± SD of three or more independent experiments. Statistical analyses were performed using the Student *t* test. $*P < 0.05$, $**P < 0.01$.

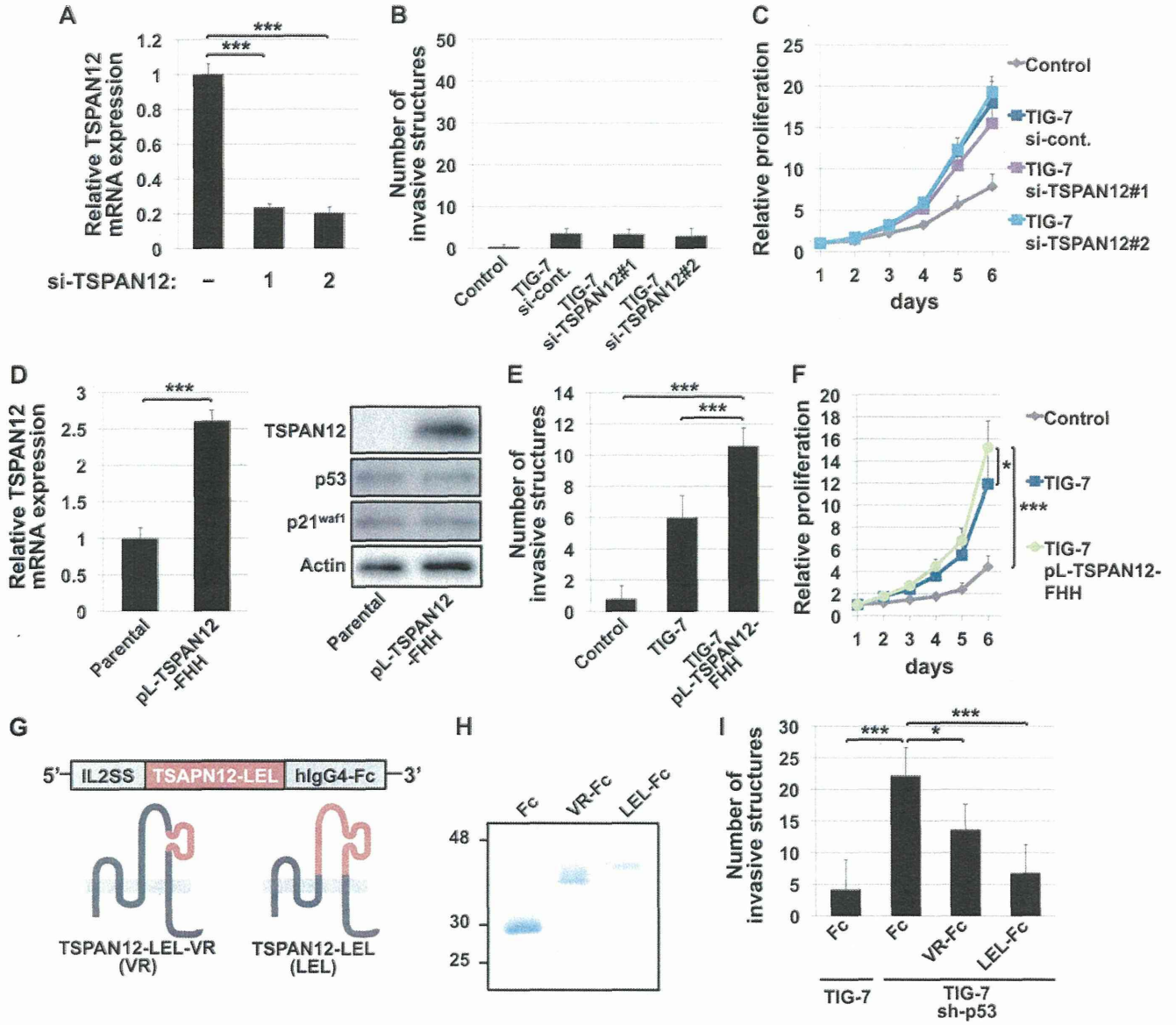

Fig. S6. TSPAN12 regulated cancer cell invasiveness and proliferation. (*A*) Efficiency of TSPAN12 knockdown in parental TIG-7 cells. Parental TIG-7 cells were transfected with control siRNAs or siRNAs against TSPAN12. Expression levels of TSPAN12 were determined by qRT-PCR. (*B*) TSPAN12 knockdown in parental TIG-7 cells did not inhibit invasiveness in H1299-GFP cells. H1299-GFP cells were cocultured with either parental TIG-7 cells or TSPAN12-depleted TIG-7 cells in Matrigel. After 4–5 d, invaded H1299-GFP cells were observed and quantified. (*C*) TSPAN12 knockdown in parental TIG-7 cells did not inhibit proliferation in H1299-LUC cells. H1299-LUC cells were cocultured with either parental TIG-7 cells or TSPAN12-depleted TIG-7 cells in 96-well plates. Luciferase activity was measured every day until day 6. (*D*) Expression levels of TSPAN12 in TIG-7 cells infected with lentiviruses with or without TSPAN12-FHH. (*E*) The overexpression of TSPAN12 in TIG-7 cells enhanced invasiveness in H1299-GFP cells. H1299-GFP cells were cocultured with either parental TIG-7 cells or TSPAN12-expressing TIG-7 cells in Matrigel. After 4–5 d, invaded H1299-GFP cells were observed and quantified. (*F*) The overexpression of TSPAN12 in TIG-7 cells enhanced proliferation in H1299-LUC cells. H1299-LUC cells were cocultured with either parental TIG-7 cells or TSPAN12-expressing TIG-7 cells in 96-well plates. Luciferase activity was measured every day until day 6. (*G*) Construction of large extracellular loops of TSPAN12. (*H*) Purified large extracellular loops of TSPAN12 were stained with CBB. (*I*) The large extracellular loops of TSPAN12 inhibited the invasiveness of H1299-GFP cells. H1299-GFP cells were cocultured with either parental TIG-7 cells or p53-depleted TIG-7 cells with indicated LELs of TSPAN12 in Matrigel. After 4–5 d, invaded H1299-GFP cells were observed and quantified. Data are the mean ± SD of three or more independent experiments. Statistical analyses were performed using the Student *t* test. $*P < 0.05$, $***P < 0.001$.